SAGBO Mechanism on High Temperature Cracking Behavior of Ni-base Superalloys

W. Carpenter, B.S.-J. Kang, and K.M. Chang

Mechanical and Aerospace Engineering Department
West Virginia University
Morgantown, WV 26506

Abstract

Many Ni-base superalloys such as Inconel 718 show a time dependent behavior of crack growth at elevated temperatures above 500°C. The environmental interaction at the crack tip plays an important role on the crack growth rate, and the stress assisted grain boundary oxidation (SAGBO) is the acting mechanism for these alloys cracking in air. In this research, the SAGBO effect on the creep crack growth behavior of fatigue pre-cracked single edge-notched (SEN) Inconel 718 specimens tested in air and oxygen-free environments is investigated. High temperature moire interferometry (HTMI) was applied to obtain in-situ crack tip displacement fields of the test specimens at 650°C under constant loading conditions. The diffusion of oxygen along grain boundaries in front of the crack tip governs the size and degree of environmental damage. The formation of a SAGBO-induced damage zone at the crack tip causes the cracking in a brittle mode as verified by our experimental results. The damage zone induces intergranular fracture and accelerates the crack growth rate. The coarsening of the damage zone is a linear function with time under given temperatures, oxygen partial pressure, and stress intensity factor.

Superalloys 718, 625, 706 and Various Derivatives
Edited by E.A. Loria
The Minerals, Metals & Materials Society, 1997

Introduction

Creep crack growth behavior in nickel-base superalloys has been widely reported to be environmentally sensitive. Creep crack growth rates can be as much as 1000 times faster in air than in vacuum or inert gaseous environment[1,2]. Additionally, the incubation time for crack growth has been show to be vastly greater in the inert environment than in air.

Two strong interactive mechanisms are responsible for much of the intergranular cracking, which is the weakest link in IN718 as well as most other nickel-base superalloys at elevated temperatures. These are slip induced intergranular cracking and oxidation assisted crack growth.[3] Some of the original theories behind oxidation assisted crack growth hypothesized that cavitation attributed to the enhanced crack growth. However, upon further research, Gao, et al.,[4] pointed out that environmentally enhanced cavitation cannot be the dominant mechanism for enhanced creep crack growth, and an alternate mechanism needs to be examined.

A new hypothesis is that the formation of oxides, possibly niobium oxide, forms on the grain boundaries ahead of the crack tip which leads to the brittle intergranular fracture, i.e. (SAGBO) embrittlement. To verify this theory, one must first explain how an abundance of niobium is present in the grain boundaries. There are several possibilities to elucidate this phenomenon. First, niobium may segregate at grain boundaries of polycrystals during heat treatment. Research has shown that it is possible to have as much as four times the amount of niobium on the grain boundaries as compared to the bulk percentage after heat treatment.[5] Also, the possible decomposition of niobium carbide particles may supply excess niobium to the grain boundary. Gao, et. al,[4] have shown that some types of niobium carbides do indeed react with the environment as evidenced by the "feathery" appearance of these carbides when viewed using a scanning electron microscope. Also, preferential formation of δ phase at the grain boundary could occur during aging.

Materials and Experimental Work

The material used for this research was INCONEL 718, a nickel-base superalloy furnished by INCO Alloys, International. The chemical composition of the bar stock used for the specimens is given in Table 1. Table 2 depicts the heat treatment given to the alloys prior to testing. Table 3 shows the typical material properties for IN718 at 650°C.

Composition	Ni	Fe	Cr	Ti	Nb	Mo	Al	C
Bar	52.9	18.8	18.4	0.91	4.97	3.0	0.53	0.04

Table 1 Chemical Composition of Received IN718

Annealed at 982°C for 1h, air cooled to room temperature
Aged at 718°C for 8h, furnace cooled to 621°C
Held at 621°C for a total aging time of 18h
Air cooled to room temperature

Table 2 Heat Treatment for IN718

Yield Strength (MPa)	Young's Modulus (MPa)	K_{th} (MPa$\sqrt{m}$)	K_{IC} (MPa$\sqrt{m}$)
1000	165,000	15	96.4

Table 3 Material Properties of IN718 at 650°C

The specimens were single edge-notched tension (SENT) and Figure 1 shows the typical specimen geometry. Table 4 gives the specific specimen dimensions for each of the test cases.

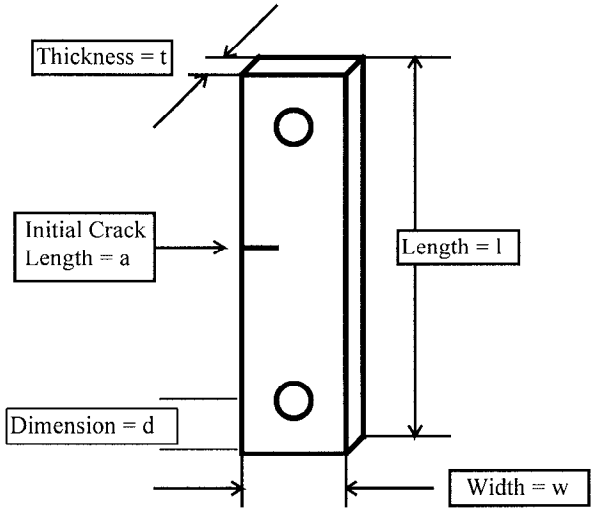

Figure 1 Specimen Geometry

Specimen	l (mm)	t (mm)	d (mm)	w (mm)	a (mm)	a/w ratio
S2	130.0	2.00	10.0	23.70	8.75	0.369
S3	140.0	1.85	10.0	24.35	13.7	0.563

Table 4 Specimen Dimensions

The test specimen was mounted inside a retort quartz tube assembly which was placed inside a furnace. This test setup has the capability of controlling the gas content in the retort tube while applying load to the test specimen at elevated temperatures. The oxygen content in the retort tube was monitored using an Illinois Instruments 3000 Oxygen Analyzer. The oxygen content was reduced by flowing research purity (99.9999%) argon to the retort quartz tube assembly and alternated with a vacuum pump down cycle. A constant load was applied after each specimen reached the final operating temperature. Flow charts depicting the testing procedures for each specimen are presented in Figures 4 and 5. Full-field v-displacements were measured using High Temperature Moire Interferometry (HTMI). Figures 2 and 3 show typical recorded moire fringe patterns of specimen S3 under inert gaseous environment (Figure 2) and 324 minutes after the introduction of oxygen (Figure 3).

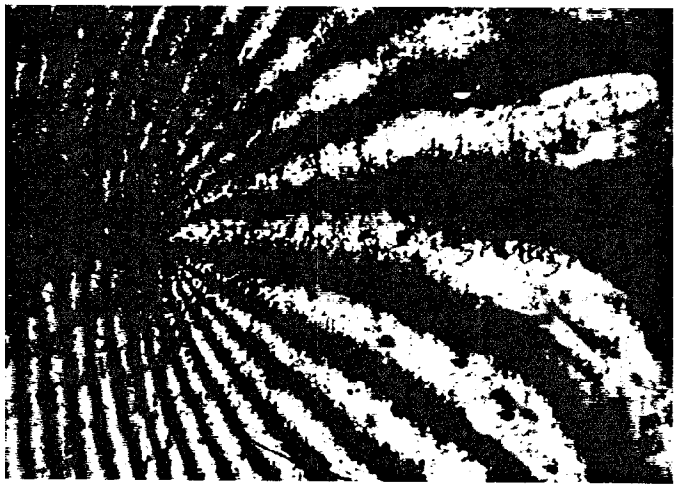

Figure 2, v-displacement, Moire Fringe Pattern, Specimen S3, T=650°C, K_I=42 MPa$\sqrt{m}$, Time = 2 days, Inert Environment.

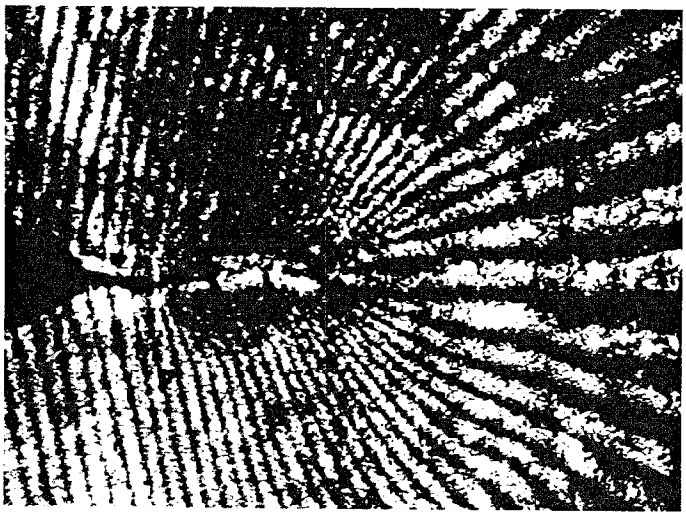

Figure 3, v-displacement, Moire Fringe Pattern, S3, T=650°C, K_I=42 MPa$\sqrt{m}$, Time = 10 days and 324 min., 324 minutes after oxygen introduction.

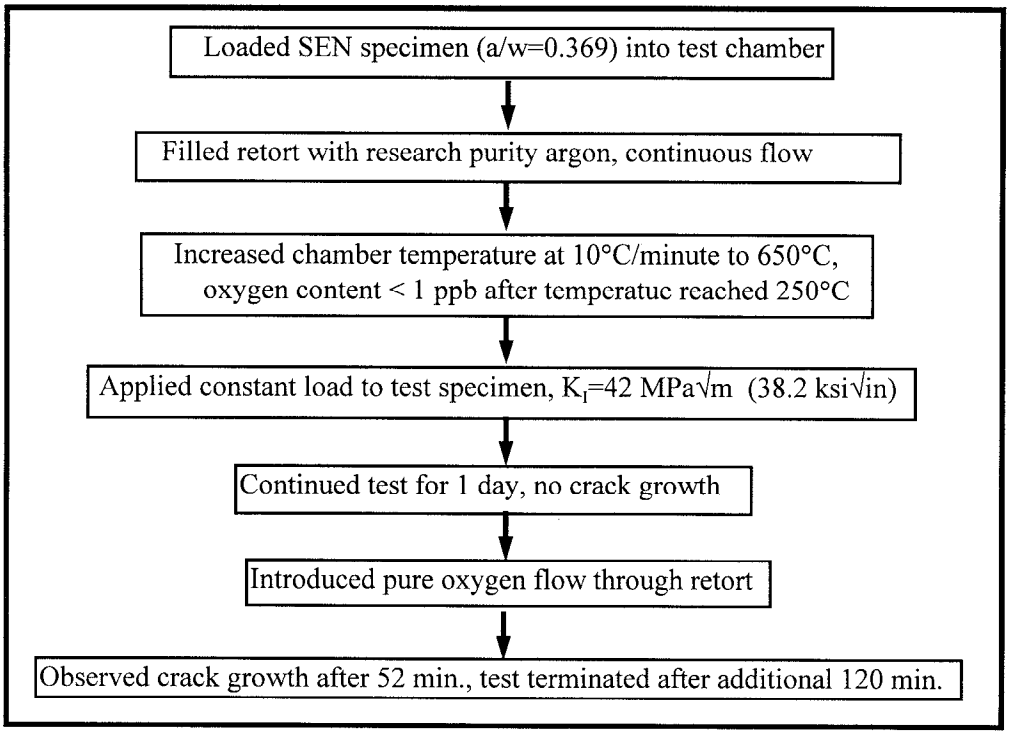

Figure 4, Testing Sequence for Specimen 2

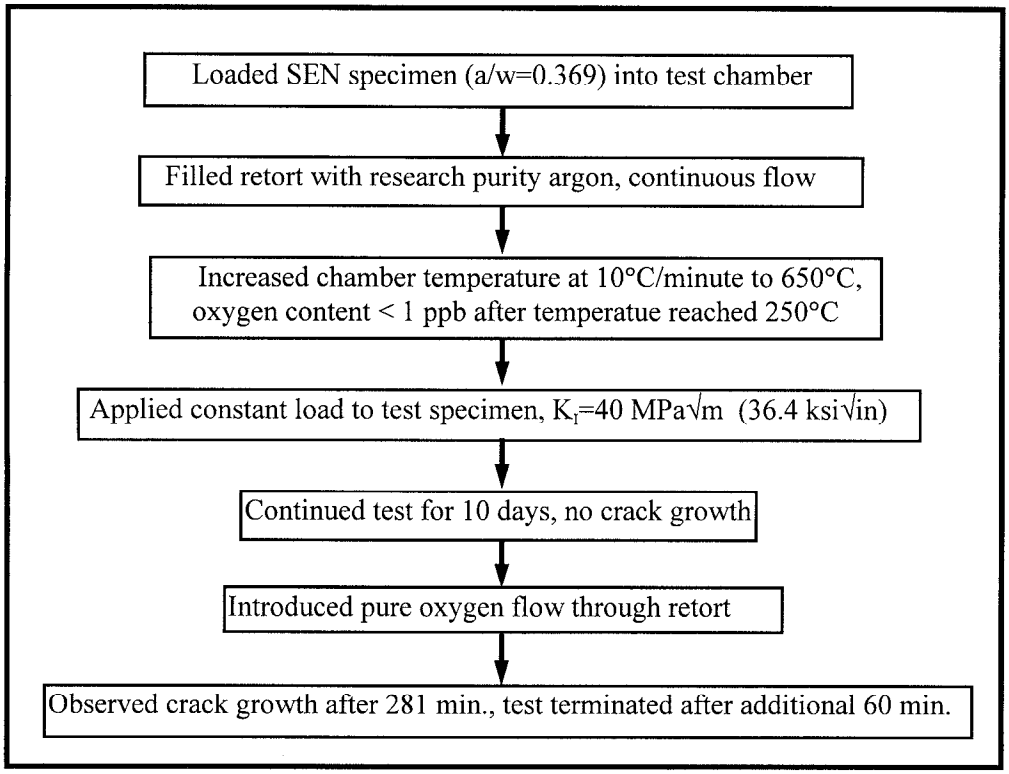

Figure 5, Testing Sequence for Specimen 3

Results and Discussion

A detailed analysis of the recorded moire fringe patterns for each specimen was performed. Based on the analysis of these images, a crack extension curve was constructed for these specimens. Figure 6 shows crack extension versus time for specimens 2 and 3. Note that the time scale starts at the initiation of crack growth. The incubation time for the creep crack growth to begin was much longer for specimen 3, possibly due to its longer aging time. Furthermore, it has been shown that creep crack growth can be correlated according to the Arrhenius relationship[6]:

$$\frac{da}{dt} = AK^n \exp\left[\frac{-Q}{RT}\right] \quad (1)$$

where a is the crack length, t is time, A is a constant, n is the slope of the log-log plot, K is the mode I stress intensity factor, Q is the activation energy, R is the universal gas constant and T is the absolute temperature. Accordingly, a plot of log (da/dt) versus log K_I was produced for each test and is presented in Figure 7. As can be seen from the graph, the Arrhenius relationship holds for these tests.

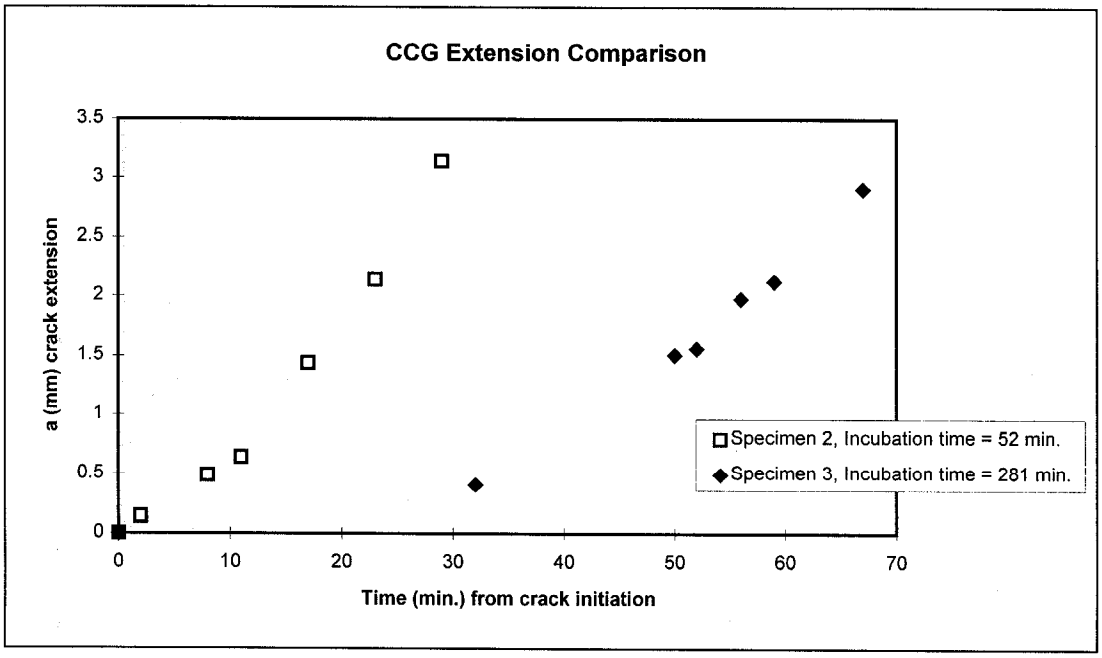

Figure 6, Creep Crack Growth of IN 718 SENT Specimen 3, T=650°C, Delayed Oxygen Atmosphere.

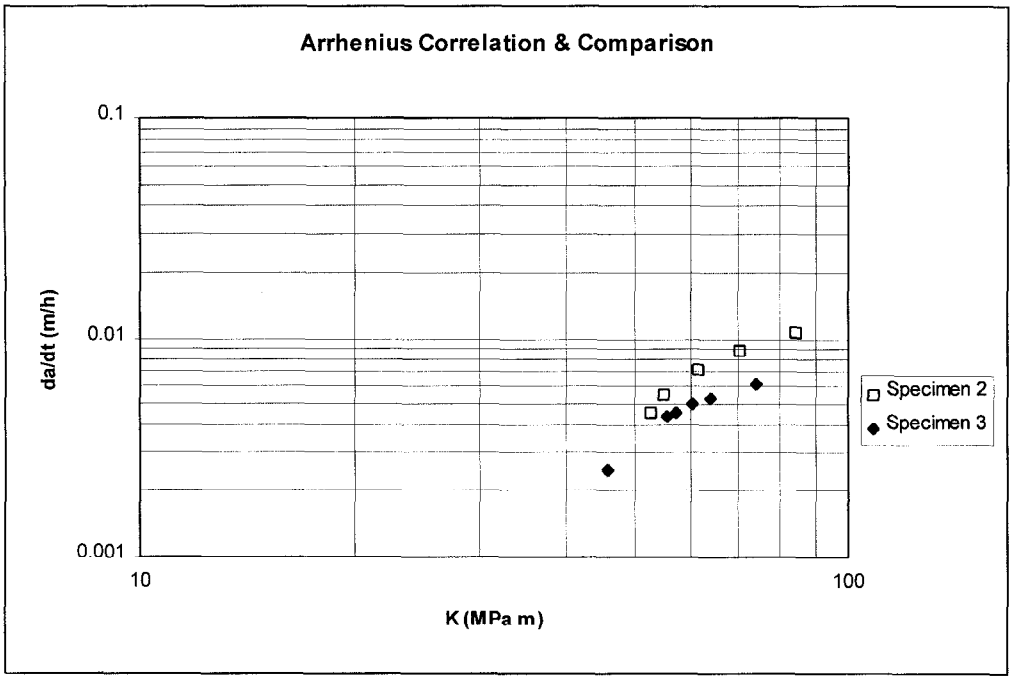

Figure 7, Arrhenius Plot Comparison,
T=650°C, Delayed Oxygen Atmosphere.

Microstructural Analysis

One major problem of studying macroscopic crack growth at the microscopic level is connecting facets of one area with those of another area. In an effort to determine the mechanism of this creep crack growth behavior, it is necessary to view the overall crack growth related to microstructural variations. Therefore, a sequence of SEM micrographs were taken and then "linked" using image manipulation software to allow for in-depth microstructural studies. Figures 8 and 9 show the overall crack growth sequence for each specimen from the end of the fatigue pre-crack to the cessation of the environmentally assisted creep crack growth. As shown in Figures 8 and 9, the evidence of SAGBO-induced intergranular crack growth is apparent.

Evidence of preferential grain boundary precipitation was clearly obtained following the analysis of each specimen. In the interests of brevity only images from specimen S3 will be reported here. Figure 10 shows the SEM micrograph of the last propagation of the crack for specimen S3. The grain boundary precipitation on the fracture path can easily be seen in this micrograph. Energy Dispersive Analysis of X-rays (EDAX) was performed on these areas of precipitates to determine their chemical composition. Both scanning EDAX mapping and point wise spectra were conducted along the fracture path that coincides with the grain boundary precipitates. A typical spectral result for an EDAX test of specimen S3 for the grain boundary precipitates as compared to matrix values is shown in Figure 11. Detailed EDAX mapping was also performed for a specific area at the end of the crack propagation. Figure 12 depicts one such scan. As can be seen from the EDAX mapping both niobium and oxygen are present in abundance on the precipitates lying in the fracture path.

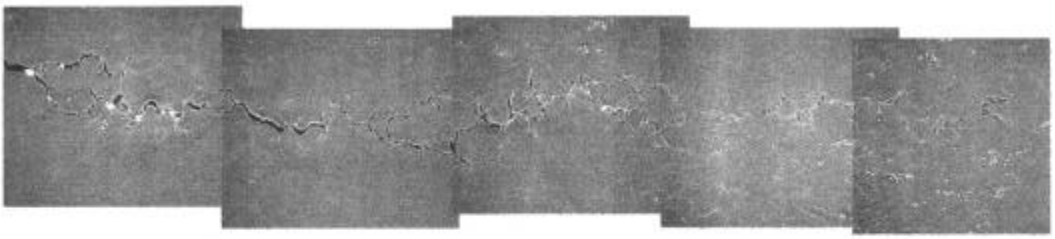

Fig. 8, SAGBO-induced creep crack growth sequence, Specimen S2.
(Micrograph taken after 30% thickness reduction)

|----------|
300 μm

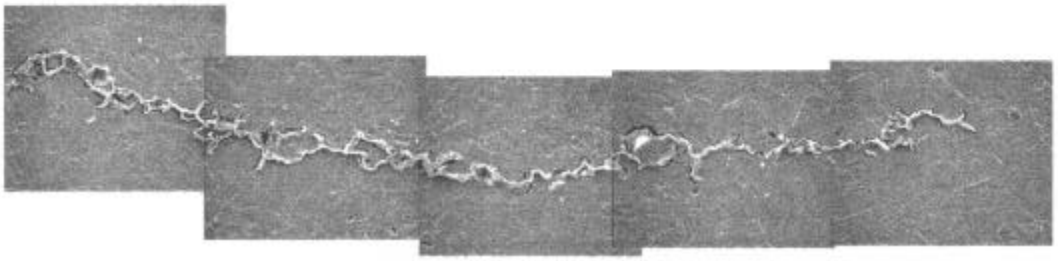

Fig. 9, SAGBO-induced creep crack growth sequence, Specimen S3.

|----------|
300 μm

Fig. 10, Enlargement of Crack Tip Region. |--------| 10 μm
(Arrow indicates particle studied)

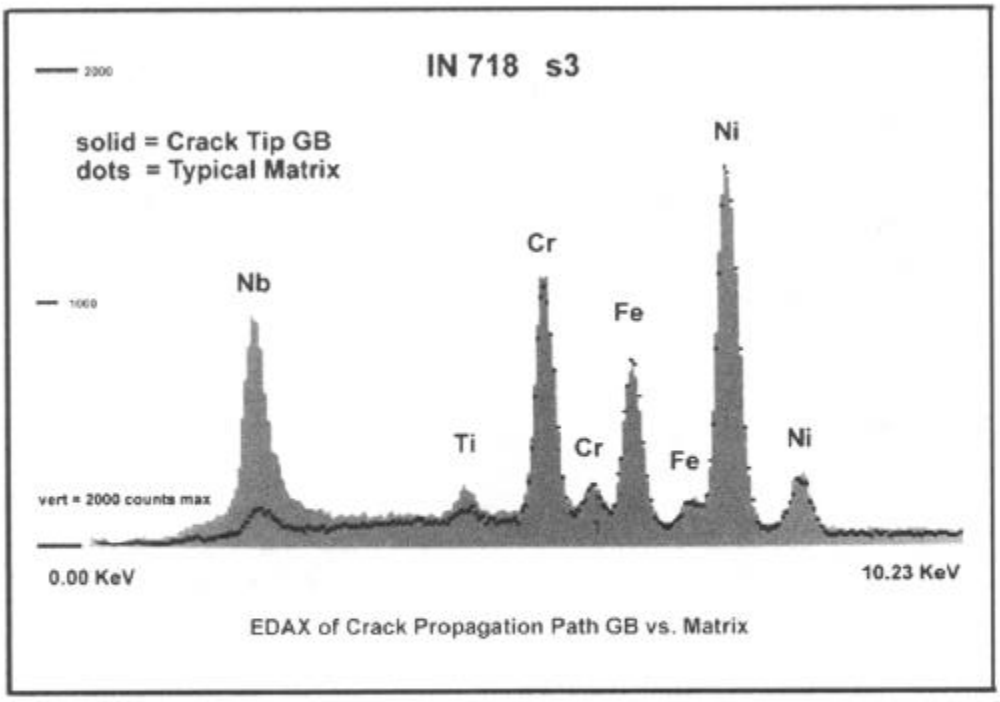

Fig. 11, EDAX Spectra of Grain Boundary Precipitation.

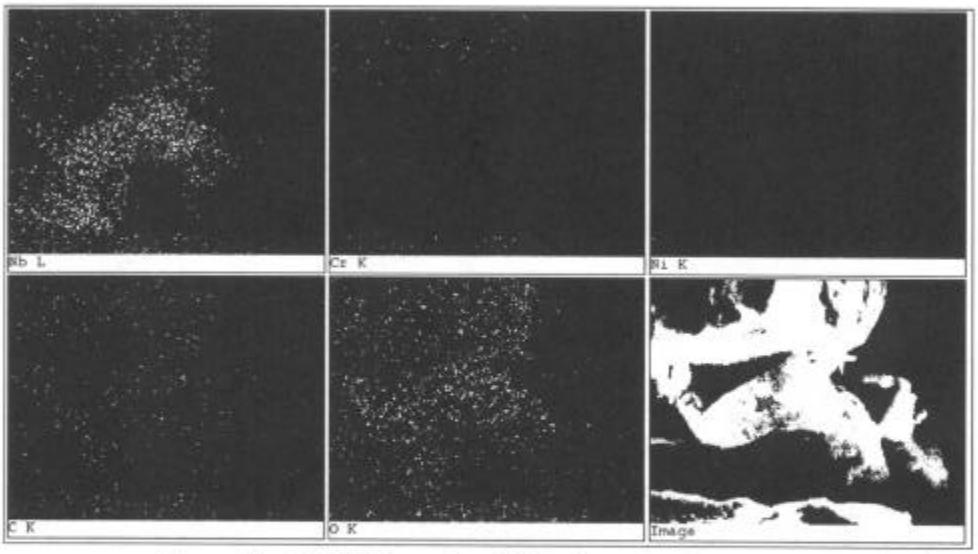

Figure12, EDAX Map of particle shown in Fig. 10 |-------| 5 um

Summary

These results clearly show that the role of niobium segregation to the grain boundaries in front of a sharp crack is important to the creep crack growth rate. It is proposed that the combination of the decomposition of large niobium carbide particles and the segregation of niobium to the grain boundaries during heat treatment allow an over-abundance of niobium to be present there. Subsequently, the formation of niobium oxide wedges results in brittle elastic intergranular fracture.

References

[1] Floreen S. and Kane, R.H., Fatigue of Engineering Materials and Structures, 2. 401-412, 1980.

[2] Strucke, M., Khobaib, M., Majumdar, B., and Nicholas, T., Advances in Fracture Research, 6, 3967-3975, 1984.

[3] Edward A. Loria, "The Status and Prospects of Alloy 718", Journal of Metals, 36-41, July 1988.

[4] M. Gao, et al., "Chemical and Microstructural Aspects of Creep Crack Growth in INCONEL 718 Alloy", Superalloys 718, 625, 706 and Various Derivatives.581-592. TMS, 1994.

[5] X.J. Pang, et al., "Surface Enrichment and Grain Boundary Segregation of Niobium in Inconel 718 Single and Poly-Crystals", Scripta Metallurgica et Materialia, Vol. 31, No. 3, 345-350, 1994.

[6] P. Valerio, M. Gao and R.P. Wei, "Environmental Enhancement of Creep Crack Growth in Inconel 718 by Oxygen and Water Vapor", Scripta Metallurgica et Materialia, Vol. 30, No. 10, 1269-1274, 1994.